Crack Propagation in Catalytic Pellets Due to Thermal Stresses

L. Boshoff-Mostert and H. J. Viljoen
Dept. of Chemical Engineering, University of Nebraska-Lincoln, Lincoln, NE 68588

Catalytic combustion reactions and reacting systems that operate in the parameter sensitivity region of the kinetic regime are likely to experience sudden temperature changes, resulting in the development of thermal stresses in the catalyst support. The unified theory of Hasselman is used to study the onset and extent of crack propagation in catalyst support media. This theory is based on the principle that cracks propagate (terminate) when the total energy of the system increases (decreases) with additional crack growth. It is shown that the total energy of the medium (elastic and fracture energy) varies with time and position in the medium, and the extent of crack growth also varies from one point to the other. Within the limitation of the assumption that the crack density is low enough, the model provides valuable insight into the durability and mechanical strength of ceramic support media.

Introduction

Although the structural failure of catalytic support media has been frequently observed in practice, very little research has been done on this topic. There are primarily three causes for the failure of ceramic-based supports. Chemical reactions between support material and processing streams cause leaching or transformation of the structure. Entrapment of volatile species in internal pores or pores with restricted access leads to internal pressure rises. Varying temperature fields in the structure results in the development of thermal stresses. The chemical attack of the structure can be overcome by a proper choice of support material, keeping in mind that the choice for a support is sometimes limited from a catalytic point of view. Steam is a notoriously difficult component to handle; apart from leaching certain components it also causes failure by entrapment in pores. Thermal stresses develop in a connected body when a temperature gradient is present. If the body has fixed boundaries, a linear temperature profile is sufficient for the development of thermal stress. Fixed boundaries are not a prerequisite; however, thermal stress can also develop in traction-free bodies.

Thiart et al. (1990, 1993) studied thermal shock in catalytic pellets, including effects of temperature-dependent physical properties on the stress fields. These studies focused on the thermal stresses and how they form due to chemical reactions. The aspects of crack formation were not addressed at all. The only criterion for mechanical failure was a comparison between the maximum tensile stress value and a breaking strength. Breaking strengths were reported by Crandall and Ging (1955) for a temperature range 20–1,200°C. Coble and Kingery (1956) reported the tensile strength of alumina at 750°C for different porosities and presented their results in the form of an empirical relation. Coble and Parikh (1972) also published an empirical expression relating the dependence of tensile strength of alumina with grain size and porosity.

A more theoretical approach to estimate the breaking strength is based on the work of Irwin (1957). He introduced the concepts of stress intensity factors and the coefficients K_I, K_{II}, and K_{III} to quantify stress concentration at crack tips under normal, transversal shear, and longitudinal shear loads. The stress intensity factors depend only on the applied loading and crack geometry, and consequently determine the intensity of the local field at the crack tip (Lawn and Wilshaw, 1975). When the K factors reach a specified maximum value, crack growth is initiated. In order to calculate the K factors it is necessary to have knowledge of existing cracks. Bahr et al. (1987) demonstrated this calculation for a single-edge cracked strip under thermal shock. The method of superposition is used; the stress fields are calculated in the absence of any cracks, then the calculation is repeated with traction boundaries imposed at the position of the crack opposite in

Correspondence concerning this article should be addressed to H. J. Viljoen.

sign to the stress values (for the stress-free case) at the crack position. Cherepanov (1979) gave several examples for two-dimensional structures (plane-strain or plane-stress problems). The problems are first formulated in terms of potentials (so-called Kolosov–Muskhelishvili potentials, which are functions of a single complex variable) before they are solved.

Griffith (1920) analyzed the stability of a crack in an elastic body. He proposed the following relation between the stress, σ_c, and crack length $\mathcal{L}$,

$$\sigma_c = \lambda_1 \sqrt{\frac{E_Y G}{\mathcal{L}}},$$

where λ_1 is a factor (for example, $\lambda_1 = \sqrt{2/\pi}$ for a plane stress state). If the stress is less than σ_c, no crack extension occurs; however, if this value is exceeded, the process of crack extension begins. The Griffith theory oversimplifies certain failure processes (cf. Cherepanov, Chaps. 5–7). Whereas this theory focuses on a single crack in a (usually semiinfinite) body, Walsh (1965) analyzed the compressibility of rocks with an existing crack distribution. He derived expressions for the change in strain energy of an elastic body due to the presence of cracks as functions of the crack density and the average crack length. Hasselman (1969) used these results to develop a fracture-mechanical theory for crack propagation in brittle ceramic bodies.

In this work we use Hasselman's theory to analyze the crack propagation in ceramic supports. The transient temperature field is the result of a jump from the kinetic state to the ignited state, and the growth of cracks is calculated for the transient stresses. It is shown that crack growth is limited for a specimen that is already cracked. Within limits a precracked specimen is actually tougher than a flawless one. This result is consistent with the results of Hasselman (1969).

Thermoelastic Model

In general, the thermoelastic model constitutes a set of coupled partial differential equations, which include an energy balance and three displacement equations. Whereas the energy balance equation is of the parabolic type, the displacement equations are hyperbolic. The inertia terms are often neglected in the latter equations, ruling out the description of shock behavior. Usually the inclusion or exclusion of inertia terms is based on a comparison of the different characteristic times that are involved in the process (Thiart et al., 1991). Inertia terms must be considered when the temperature changes occur on a time scale that is comparable with the time scale for the propagation of mechanical perturbations. Often chemical reactions occur on a slower time scale than the acoustic time scale, and the displacement equations become elliptic. The equations are coupled due to thermoelastic dissipation. This term is negligible compared to other source terms in the energy balance (Boley and Weiner, 1960, p. 44) and if it is dropped from the energy balance, the equations are uncoupled. The energy balance can be solved, and temperature merely plays the role of a parameter in the displacement equations.

The support medium that we will analyze is a spherical pellet of radius R. Properties consistent with λ-alumina will be used. A first-order chemical reaction is chosen for this study; we also limit the reaction to a thin zone at the surface of the pellet. This restriction permits an analytical solution of the temperature and subsequently a clearer presentation of the stress and strain tensors. It is straighforward to modify the model for other reaction(s) and to apply the theory of crack propagation for those changes. The energy balance is given by

$$\rho_s C p_s \frac{\partial T}{\partial t} = k_s \nabla T, \tag{1}$$

and at $r = R$ the following condition holds,

$$h(T - T_b) + k_s \frac{dT}{dr} = (-\Delta H) C_s k_o e^{-E/(R_g T)}. \tag{2}$$

The species balance for C is given by

$$k_g (C_b - C_s) = C_s k_o e^{-E/(R_g T)}. \tag{3}$$

After substituting for C_s from Eq. 3 into Eq. 2, the boundary condition at $r = R$ can be written as

$$h(T - T_b) + k_s \frac{dT}{dr} = \frac{(-\Delta H) k_o k_g C_b e^{-E/(R_g T)}}{k_g + k_o e^{-E/(R_g T)}}. \tag{4}$$

The thermal gradient in the pellet is zero when the solution is stationary. To illustrate the crack model, we choose the parameters such that multiple solutions exist, since we are interested in the development of thermal stresses when the system jumps from the kinetic state to the ignited state. The kinetic (extinguished) stationary solution is $T = T_E = 404$ K. Suppose a perturbation causes the system to ignite. The ignited solution is $T = T_I = 800$ K.

Define the following dimensionless variables, $\rho = r/R$, $\theta = T/T_b$, and $\tau = (\kappa/R^2)t$. Equations 1 and 4 can be written in the nondimensional form:

$$\frac{\partial \theta}{\partial \tau} = \nabla \theta \tag{5}$$

$$\theta - 1 + \alpha_1 \frac{d\theta}{d\rho} = \frac{\alpha_2 e^{\gamma(\theta-1)/\theta}}{1 + \alpha_3 e^{\gamma(\theta-1)/\theta}} \qquad \rho = 1. \tag{6}$$

To permit an analytical (and thus more illustrative) solution of the stress problem, we consider an ignition process that occurs on a much shorter time scale than conduction. The initial temperature in the pellet is equal to T_E. $\theta_E = T_E/T_b$ is the lower stable root of Eq. 6 and $\theta_I = T_I/T_b$ is the upper root of Eq. 6. The jump to the ignited state is almost instantaneous, measured in the time scale of τ. This jump can be approximated by the following analytical function:

$$T(r,0) = T_E + (T_I - T_E) \frac{\sinh(\delta r)}{r \sinh(\delta)}, \tag{7}$$

where δ is a large parameter.

The solution of Eq. 5 is

$$\theta = \theta_I - (\theta_I - \theta_E) \sum_{i=1}^{\infty} A_i \frac{\sin(i\pi\rho)}{\rho} e^{-i^2\pi^2\tau} \tag{8}$$

where the coefficients A_i are defined as

$$A_i = \frac{-2\cos(\pi i)}{\pi i}.$$

The development of the temperature field in the pellet is shown in Figure 1.

Several different formulations can be used for the linear thermoelastic problem; however, we prefer to use the displacement formulations for this problem. The displacement vector $U = (u, v, w)$ describes the displacement of a point in the sphere that was originally at $P = (\rho, \theta, \phi)$ to $P + U$. Since the temperature is only dependent on one spatial variable ρ, symmetry is preserved with respect to the other spatial variables, and the displacements v and w are constants. The displacement equation for u can be written as

$$(\lambda + 2\mu) \frac{d}{d\rho} \left(\frac{1}{\rho^2} \frac{d(u\rho^2)}{d\rho} \right) - (3\lambda + 2\mu)\beta T_b \frac{d\theta}{d\rho} = 0. \tag{9}$$

In an isotropic connected medium, there are two physical properties that describe the elastic behavior, namely the Young's modulus (E_Y) and the Poisson ratio (ν). The Lame constants represent the same physical properties, defined as

$$\lambda = \frac{\nu E_y}{(1+\nu)(1-2\nu)},$$

$$\mu = \frac{E_Y}{2(1+\nu)}.$$

Integrating Eq. 9 twice, the displacement can be written as

$$u = \left(\frac{3\lambda + 2\mu}{\lambda + 2\mu} \right) \beta T_b \left[\frac{\rho\theta_I}{3} - (\theta_I - \theta_E) \right] \times \left\{ \sum_{i=1}^{\infty} A_i \left[-\frac{\cos(\pi i\rho)}{\rho\pi i} + \frac{\sin(\pi i\rho)}{\pi^2 i^2 \rho^2} \right] e^{-\pi^2 i^2 \tau} \right\} + \frac{C\rho}{3}, \tag{10}$$

where C is an integration constant that must still be determined.

Remark. The integration constant is determined by the condition that the radial stress is zero at $\rho = 1$. In a sense the term "constant" is a misnomer, since the value of C changes with time, but one should keep in mind that time plays the role of a parameter in the displacement formulation.

The normal strains are given by

$$\epsilon_{\rho\rho} = \frac{du}{d\rho} \tag{11}$$

$$\epsilon_{\phi\phi} = \epsilon_{\theta\theta} = \frac{u}{\rho}. \tag{12}$$

The resulting normal stresses are

$$\sigma_{\rho\rho} = \lambda \left(\frac{du}{d\rho} + 2\frac{u}{\rho} \right) + 2\mu \frac{du}{d\rho} - (3\lambda + 2\mu)\beta T_b \theta(\rho, \tau) \tag{13}$$

$$\sigma_{\phi\phi} = \sigma_{\theta\theta} = \lambda \left(\frac{du}{d\rho} + 2\frac{u}{\rho} \right) + 2\mu \frac{u}{\rho} - (3\lambda + 2\mu)\beta T_b \theta(\rho, \tau). \tag{14}$$

The shear stresses are zero.

The radial and angular stresses are shown in Figures 2 and 3, and are associated with the temperature field of Figure 1.

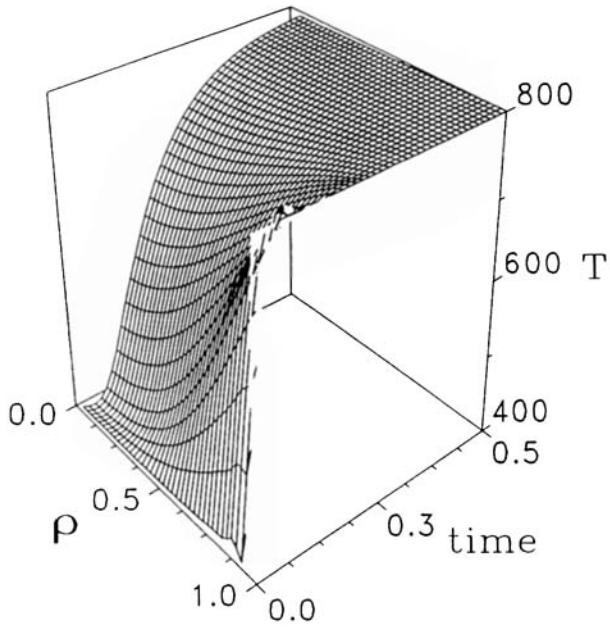

Figure 1. Temperature field.

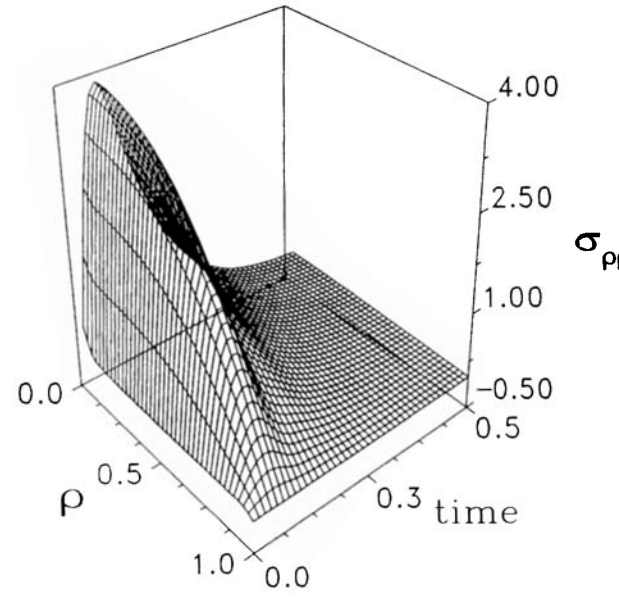

Figure 2. Radial stress field.

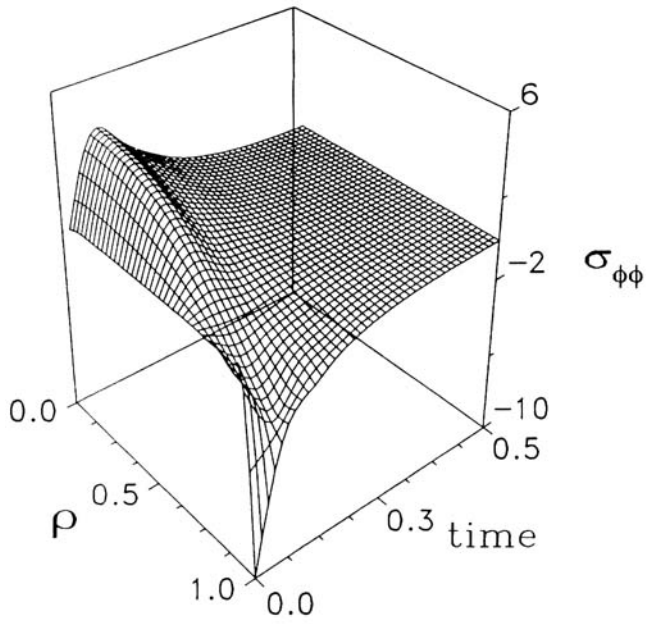

Figure 3. Angular stress field.

No external force or tractions are applied and stresses are the result of the temperature gradient only. As time progresses, the temperature gradient decreases and the pellet eventually reaches an isothermal state. The strain tensor can be easily calculated from the compatibility equations, Eqs. 11–12, and in Figure 4 the radial strain is shown. In contrast to the radial stress, the radial strain has a maximum at the free surface.

Crack Model

The pioneering work of Griffith (1920) paved the way for a more scientific approach toward the propagation of cracks and the stability of crack growth and fracture. Griffith's analysis is based on the energy of the structure, and he proposed that a crack would propagate when propagation caused a reduction in the total energy of the system. Crack propagation causes a reduction in the strain energy, but also creates new surfaces that have surface energy. One way to state the Griffith criterion is that a crack will propagate when the decrease in elastic strain energy is at least equal to the energy needed to create the new surfaces associated with the crack (Caddell, 1980). Hasselman (1969) used this concept to develop a theory for thermal shock crack initiation and crack propagation in brittle materials. These two aspects were usually examined isolation, and Hasselman's contribution lies in the unification of the two. First we define the elastic energy of the medium; in our case, it is the catalyst pellet (cf. Boley and Weiner, 1960, p. 263):

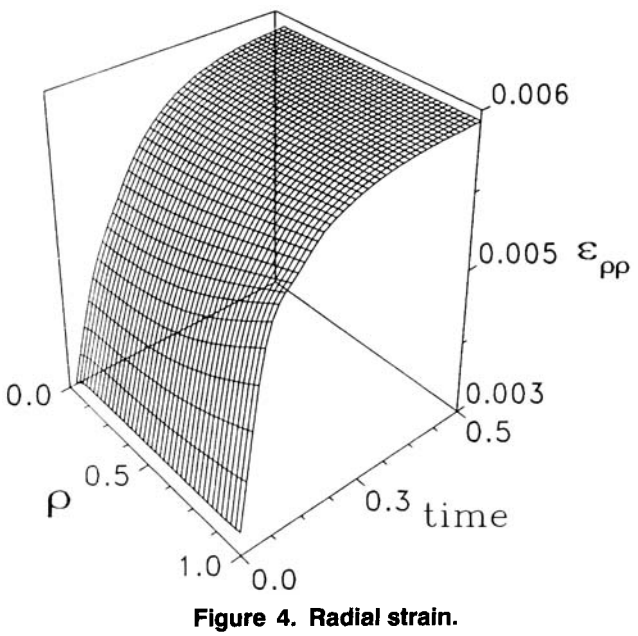

Figure 4. Radial strain.

$$W_E = \frac{1}{2}[\epsilon_{rr}\sigma_{rr} + 2\epsilon_{\theta\theta}\sigma_{\theta\theta}]. \tag{15}$$

The stress and strain fields were calculated in the previous section, and they can be expressed as functions of ρ and τ, with parameters λ and μ.

During manufacturing small cracks form in the ceramic body. Even in the unlikely event that a flawless specimen has been manufactured, cracks will form during usage. It is practical to assume that a crack distribution is present in these pellets. The size distribution of the cracks and their position in the ceramic body depends on the manufacturing process, handling, and more important, the history of the specimen, that is, the treatment it has been subjected to prior to the current analysis. For the sake of this work we assume that a known crack density is present in the pellet. The distribution is lumped and we use an average crack length $\mathfrak{L}$. (It is possible to include a distribution of crack lengths in the model.) If the crack density is uniform, we can express it as N cracks/cm^3, with average length $\mathfrak{L}$ cm. (A cm scale is used to make cross-referencing with Hasselman's work easier.) It is further assumed that the density is low enough so that cracks do not interfere with each other. Sack (1946) has shown that the Young's modulus for a cracked body is lower than the value for a flawless specimen. The exact factor depends on the form of the crack; in the case of penny-shaped cracks, which are most often used, the Young's modulus becomes

$$E_Y = E_{Y_o}\frac{9(1-2\nu)}{9(1-2\nu)+16(1-\nu^2)N\mathfrak{L}^3}, \tag{16}$$

where E_{Y_o} is the value for a flawless specimen and ν is the Poisson ratio. The Lame constants λ and μ depend on the crack distribution and average crack length as follows:

$$\lambda = \lambda_o\frac{9(1-2\nu)}{9(1-2\nu)+16(1-\nu^2)N\mathfrak{L}^3}$$

$$\mu = \mu_o\frac{9(1-2\nu)}{(1-2\nu)+16(1-\nu^2)N\mathfrak{L}^3}.$$

Substituting these forms of the Lame constants into Eqs. 13 and 14, it becomes apparent how the crack density and crack

length are related to the stress and hence the temperature field.

The fracture energy of penny-shaped cracks is

$$W_F = 2\pi N \mathfrak{L}^2 G, \tag{17}$$

where G is the surface energy of the crack face (J/cm^2). Cherepanov (1979) discussed several different methods to estimate the surface energy. The total energy of the catalyst pellet is

$$W_T = W_E + W_F. \tag{18}$$

An analytical expression of $W_T = W_T(\mathfrak{L})$ is now available and we can determine the locus of neutral stability defined by

$$\frac{dW_T}{d\mathfrak{L}} = 0. \tag{19}$$

This locus marks the transition from a region of stability to a region of unstable crack growth.

If we substitute the stress and strain fields from Eqs. 11–14 into Eq. 15 and add the fraction energy, the total energy is

$$W_T = \frac{1}{2}\left\{\frac{du}{d\rho}\left[\lambda\left(\frac{du}{d\rho}+2\frac{u}{\rho}\right)+2\mu\frac{du}{d\rho}-(3\lambda+2\mu)\beta T_b\theta(\rho,\tau)\right]\right.$$
$$\left.+2\frac{u}{\rho}\left[\lambda\left(\frac{du}{d\rho}+2\frac{u}{\rho}\right)+2\mu\frac{u}{\rho}-(3\lambda+2\mu)\beta T_b\theta(\rho,\tau)\right]\right\}$$
$$+2\pi N\mathfrak{L}^2 G. \tag{20}$$

Both Lame constants are linear in $E_Y = E_Y(\mathfrak{L})$, and we can differentiate Eq. (20) with respect to $\mathfrak{L}$ and set it equal to zero;

$$\frac{1}{2}\left\{\frac{du}{d\rho}\left[\lambda_o\left(\frac{du}{d\rho}+2\frac{u}{\rho}\right)+2\mu_o\frac{du}{d\rho}-(3\lambda_o+2\mu_o)\beta T_b\theta(\rho,\tau)\right]\right.$$
$$\left.+2\frac{u}{\rho}\left[\lambda_o\left(\frac{du}{d\rho}+2\frac{u}{\rho}\right)+2\mu_o\frac{u}{\rho}-(3\lambda_o+2\mu_o)\beta T_b\theta(\rho,\tau)\right]\right\}$$
$$\times\frac{432\mathfrak{L}^2(1-\nu^2)(1-2\nu)}{[9(1-2\nu)+16(1-\nu^2)N\mathfrak{L}^3]^2}=4\pi N\mathfrak{L}G. \tag{21}$$

This is a sixth-order polynomial that must be solved at every point in ρ and at every moment in time. There is no existing analytical method to solve general sixth-order polynomials (as was shown by Abel in 1826) and the roots are found by a numerical procedure.

Results

The elastic properties (Coble and Kingery, 1956), operating conditions, and the value for G (Hasselman, 1969) are listed in Table 1. In addition we have to specify the crack density, N. It is expected that in most cases this parameter is distributed, varying with position; however, a constant value is used in this study. In Figures 5 and 6 and Figures 7 and 8 crack densities of 1 and 2 (cracks/cm^3) are used, respectively. Since $\mathfrak{L} = \mathfrak{L}(\rho,\tau)$, we present the roots of Eq. 21 as functions of ρ at different points in time (τ). It must be pointed out that Eq. 21 does not always have positive real roots, but if positive roots exist, they are found in pairs. We denote the smaller and larger positive roots as $\mathfrak{L}_1$ and $\mathfrak{L}_2$, respectively. In Figure 5 the roots are shown at $\tau = 0.04$, 0.06, and 0.08, and 0.1. At $\tau = 0.04$, roots exist for $0 \le \rho \le 0.4$, and no roots exist for $\rho > 0.4$. The physical interpretation of this result is that crack extension can only occur at radial positions where roots exist. As time progresses, the region of crack growth is reduced. It is noted from Figure 5 that the dynamic region is limited to $0 \le \rho \le 0.3$ when $\tau = 0.10$.

Table 1. Parameter Values

Item	Value	Item	Value
C_b	10 mol/m^3	k_s	5 W/m·k
C_p	1,225 J/kg·K	r	0.01 m
G	3.5×10^{-3} J/cm^2	T_b	400 K
h	50 W/m^2·K	γ	25
ΔH	2.8×10^5 J/mol	λ	507 MPa
k_g	2.5×10^{-3} W/m·K	μ	1,173 MPa
k_o	2×10^6 m/s	ν	0.15

The crack growth process can be analyzed in the following way. An initial crack length is present, as discussed earlier. Let us define this initial length (taken as the same everywhere in the pellet) as $\mathfrak{L}_0$. If we explain the process in discrete terms, consider the roots $\mathfrak{L}_1$ at a short time later, say $\tau = \tau_1$. If $\mathfrak{L}_0 \ge \mathfrak{L}_1$, that crack is dynamically unstable and it grows; if $\mathfrak{L}_0 \le \mathfrak{L}_1$, that crack is not in the unstable region and it does not grow. Cracks that lie in the unstable region grow until they cross the value of the second root, $\mathfrak{L}_2$ (i.e., leave the unstable region). However, the crack does not stop growing immediately because it still has kinetic energy when

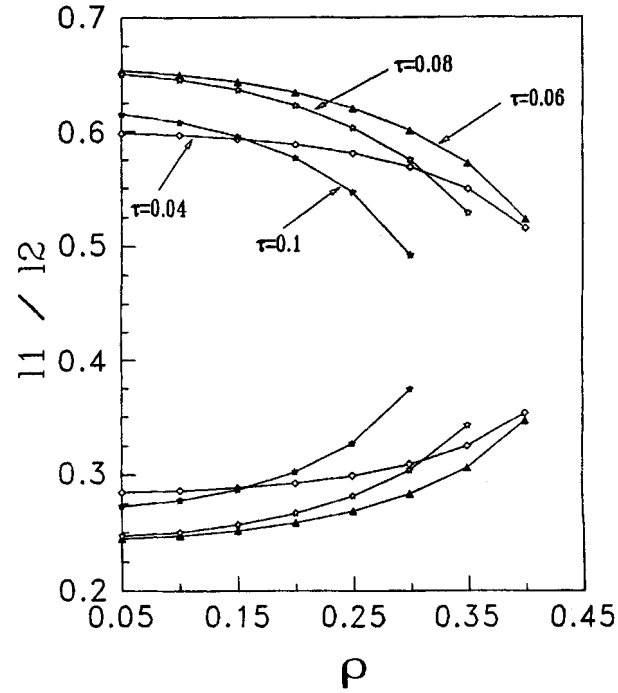

Figure 5. Roots of Eq. 21 for $N = 1$ cracks/cm^3.

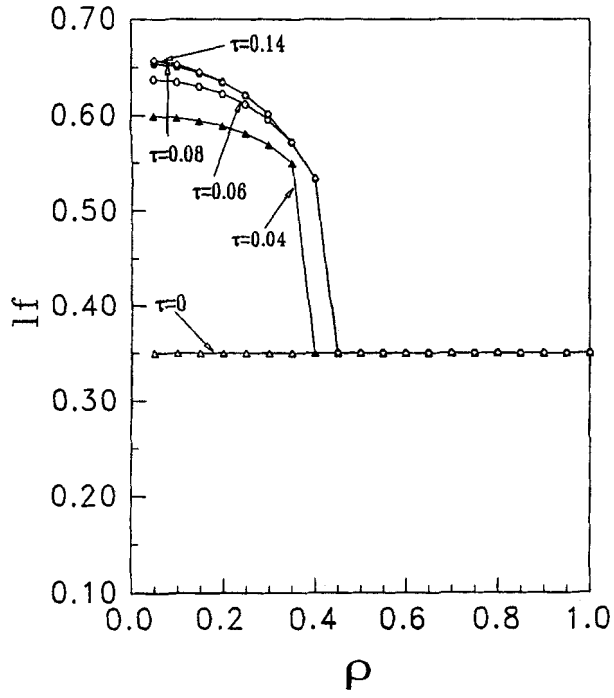

Figure 6. Crack distributions for $N = 1$ cracks/cm^3.

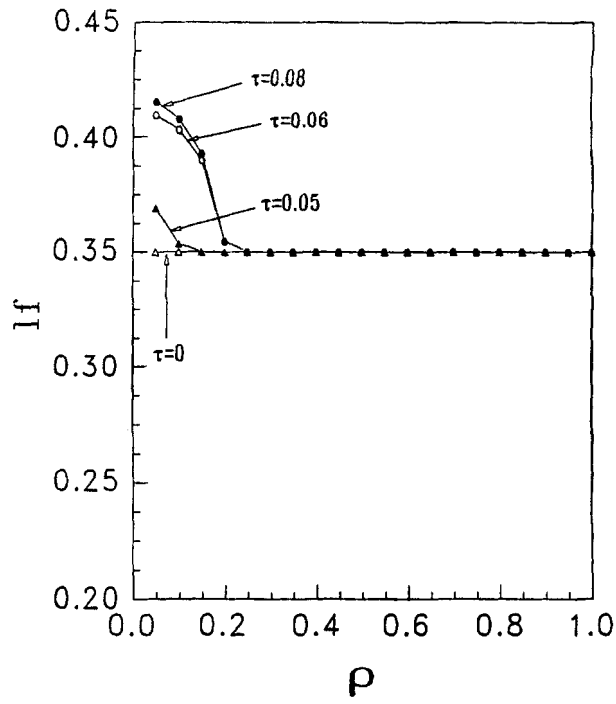

Figure 8. Crack distributions for $N = 2$ cracks/cm^3.

it enters the stable region. The crack continues to grow until a final length $\mathcal{L}_f$ is reached. This length is calculated from

$$W_T(\mathcal{L}_0) = W_T(\mathcal{L}_f). \tag{22}$$

The values $\mathcal{L}_f(\rho)$ form the crack distribution at τ_1. These values are now compared to the roots $\mathcal{L}_1$ at the next time step to determine which cracks are stable and which are not.

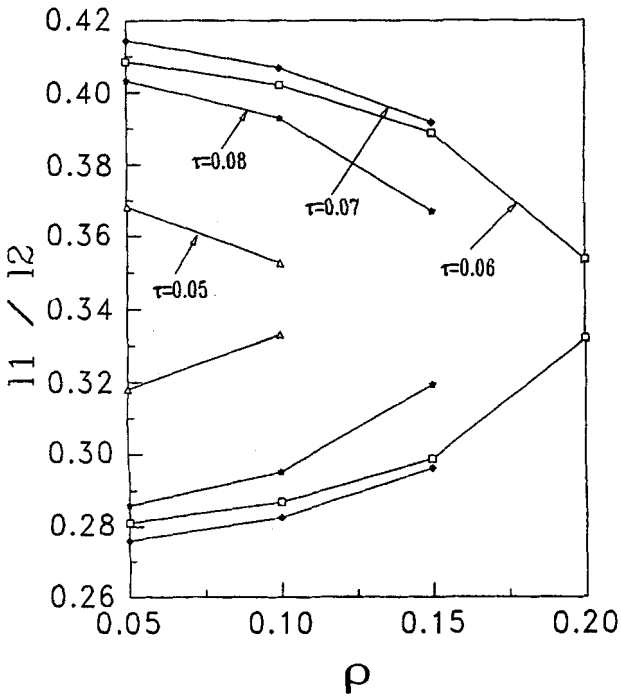

Figure 7. Roots of Eq. 21 for $N = 2$ cracks/cm^3.

The crack process can be followed as a function of time in this way. In Figure 6 the crack distribution $\mathcal{L}_f$ is shown. Note that the initial crack distribution is $\mathcal{L}_0 = 0.35$. At the time $\tau = 0.04$, the initial cracks at $0 \le \rho \le 0.4$ have grown to values ranging between 0.6 and 0.55. Further growth of cracks with time is also shown. The final crack distribution is the same as the one associated with $\tau = 0.14$.

The region of crack growth is considerably smaller when the crack density is increased to $N = 2$ (cracks/cm^3) by comparison of Figures 5 and 7. The final crack distribution for $N = 2$ is also more contained at the center of the pellet compared to the first case $N = 1$, as shown in Figure 8. The final lengths of the cracks are also considerably shorter than in the case where $N = 1$. The important conclusion is that specimens that are more precracked withstand thermal stress loads far better than specimens with a lower initial crack density. This result is consistent with the findings of Hasselman (1969), Bahr et al. (1987), and Bahr and Weiss (1986). At first glance this result may appear anomalous, since a specimen with more cracks is intuitively weaker. The dominant factor is the role that crack density plays in lowering the Young's modulus, and therefore lowering in the total elastic energy. Of course, there is a limit beyond which an increased crack density will weaken the structure, but the current analysis does not address crack interaction and the estimation of this upper limit. A distinction should be drawn between the number of cracks per volume unit (N) and the average crack length ($\mathcal{L}_0$). When N is increased, the crack growth region is smaller and cracks are sooner arrested. If the initial crack length is decreased, the onset of crack growth is delayed or possibly prevented.

When the surface energy is increased, the crack growth is drastically impeded; for example, if $G = 4.5$ J/cm^2 is used, no region is found for the current ignition process. Ceramic structures with large fracture energies will be better suited

for severe thermal loadings. The durability of cordierite (used for the manufacturing of monoliths) can be ascribed to this aspect.

Conclusions

The development of thermal stresses in a catalyst pellet has been analyzed. When the reacting system is perturbed and the ignition state becomes stable, strong temperature gradients develop that lead to transient stress-and-strain fields. Considering the pellet as an elastic sphere, it is possible to calculate transient elastic energy during the ignition process. A criterion for the onset of crack growth is presented and the locus of the region changes in the pellet as time progresses. When the lower limit of this region is compared to the existing crack lengths, it can be determined if an existing crack will begin to grow or not. A procedure to follow the development of crack growth is also presented. An important result is the ability of a system with more cracks to arrest further crack growth, reduce the overall elastic energy buildup during loading, and actually enhance the mechanical durability of the pellet.

This analysis can form the basis for future studies on other structures that are thermally loaded, such as, catalytic monoliths, porous burners, and burner supports. The susceptibility of flawless or near-flawless specimens to severe or catastrophic crack growth juxtaposed to the enhanced durability of cracked specimens strongly suggests that the intentional introduction of cracks during the manufacturing phase is a way to make more durable structures. However, the length of initial cracks must be kept small; as long as $\mathcal{L}_0 < \mathcal{L}_1$, no crack growth occurs.

Acknowledgment

The authors gratefully acknowledge the financial support of the National Science Foundation through grant CTS-9308813.

Notation

C = concentration, mol/m^3
C_b = concentration in bulk gas, mol/m^3
C_s = concentration at pellet surface, mol/m^3
Cp_s = specific heat capacity, J/kg·k
E = activation energy, J/mol
ΔH = heat of reaction, J/mol
h = heat transfer coefficient, W/m^2·K
k_g = thermal conductivity of gas, W/m·K
k_o = frequency factor, m/s
k_s = thermal conductivity of pellet, W/m·K
R_g = universal gas constant, J/mol·K
T = temperature, K
t = time, s
U = displacement vector, m

Greek letters

$\alpha_1 = k_s/hR$
$\alpha_2 = (-\Delta H)k_o C_{bo} e^{-\gamma}/hT_b$
$\alpha_3 = k_o e^{-\gamma}/k_g$
β = coefficient of linear thermal expansion, 1/°C
$\gamma = E/R_g T_b$
θ = dimensionless temperature, T/T_b
κ = thermal diffusivity, $k_s/\rho_s Cp$
ρ = dimensionless radius r/R
ρ_s = density of pellet, kg/m^3

Subscripts

b = bulk
$\theta\theta$ = angular
$\rho\rho$ = radial
$\phi\phi$ = azimuthal

Literature Cited

Abel, N. H., "On the Impossibility of a General Solution of Equations of Higher Degree Than the Fourth," *J. für die Reine und Angewandte Mathematik*, Vol. 1, Article 8, Berlin (1826).

Bahr, H.-A., H. Balke, M. Kuna, and H. Liesk, "Fracture Analysis of a Single Edge Cracked Strip under Thermal Shock," *Theor. Appl. Fract. Mech.*, **8,** 33 (1987).

Bahr, H.-A. and H.-J. Weiss, "Heuristic Approach to Thermal Shock Damage Due to Single and Multiple Crack Growth," *Theor. Appl. Fract. Mech.*, **8,** 57 (1986).

Boley, B. A., and J. H. Weiner, *Theory of Thermal Stresses*, Wiley, New York (1960).

Caddell, R. M., *Deformation and Fracture of Solids*, Prentice Hall, Englewood Cliffs, NJ (1980).

Cherepanov, G. P., *Mechanics of Brittle Fracture*, McGraw-Hill, New York (1979).

Coble, R. L., and W. D. Kingery, "Effect of Porosity on Physical Properties of Sintered Alumina," *J. Amer. Ceram. Soc.*, **39,** 377 (1956).

Coble, R. L., and N. M. Parikh, "Fracture in Polycrystalline Ceramics," *Fracture. An Advanced Treatise*, Vol. VII, H. Liebowitz, ed., Academic Press, New York (1972).

Crandall, W. B., and J. Ging, "Thermal Shock Analysis of Spherical Shapes," *J. Amer. Ceram. Soc.*, **38,** 44 (1955).

Griffith, A. A., "The Phenomena of Rupture and Flow in Solids," *Phil. Trans. Roy. Soc.*, **A221,** 163 (1920).

Hasselman, D. P. H., "Unified Theory of Thermal Shock Fracture Initiation and Crack Propagation in Brittle Ceramics," *J. Amer. Ceram. Soc.*, **52,** 600 (1969).

Irwin, G. R., "Analysis of Stresses and Strains Near the End of a Crack Traversing a Plate," *J. Appl. Mech.*, **24,** 361 (1957).

Lawn, B. R., and T. R. Wilshaw, *Fracture of Brittle Solids*, Cambridge Univ. Press, Cambridge, England (1975).

Sack, R. A., "Extension of Griffith's Theory of Rupture to Three Dimensions," *Proc. Phys. Soc. London, A*, **58,** 729 (1946).

Thiart, J. J., H. J. Viljoen, K. Kriel, J. Puszynski, J. E. Gatica, and V. Hlavacek, "Development of Thermal Stresses in Reacting Media: I. Failure of Catalyst Particle," *Chem. Eng. Sci.*, **46,** 351 (1991).

Thiart, J. J., S. M. Bradshaw, H. J. Viljoen, and V. Hlavacek, "Thermochemical Stress Development in Ceramic Catalyst Supports," *Chem. Eng. Sci.*, **48,** 1925 (1993).

Walsh, J. B., "The Effect of Cracks on the Compressibility of Rock," *J. Geophys. Res.*, **70,** 381 (1965).

Manuscript received Aug. 7, 1995, and revision received Nov. 15, 1995.